Optimization and Energy Management of Hybrid Photovoltaic-Diesel-Battery System to Pump and Desalinate Water at Isolated Regions

HEGAZY REZK [1,2], **MUJAHED AL-DHAIFALLAH** [3], **(Member, IEEE),**
YAHIA B. HASSAN [4], **AND HAMDY A. ZIEDAN** [5]

[1]College of Engineering at Wadi Addawaser, Prince Sattam Bin Abdulaziz University, Al-Kharj 11911, Saudi Arabia
[2]Electrical Engineering Department, Faculty of Engineering, Minia University, Minya 61517, Egypt
[3]Systems Engineering Department, King Fahd University of Petroleum and Minerals, Dhahran 31261, Saudi Arabia
[4]Electrical Engineering Department, Higher Institute of Engineering, Minya 61517, Egypt
[5]Electrical Engineering Department, Faculty of Engineering, Assiut University, Asyut 71518, Egypt

Corresponding authors: Hegazy Rezk (hegazy.hussien@mu.edu.eg) and Mujahed Al-Dhaifallah (mujahed@kfupm.edu.sa)

ABSTRACT This research work aims to provide detailed feasibility, a techno-economic evaluation, and energy management of stand-alone hybrid photovoltaic-diesel-battery (PV/DG/B) system. The proposed system can be applied to supply a specific load that is far away from the utility grid (UG) connection, and it is located in Minya city, Egypt, as a real case study. The daily required desalinated water is 250 m^3. The total brackish water demands are 350-500 m^3 and 250-300 m^3 of water in summer and winter seasons, respectively. Two different sizes of reverse osmosis (RO) units; RO-250 and RO-500, two energy control dispatch strategies; load following (LF) and cycle charging (CC); two sizes of DG; 5 kW and 10 kW are considered in the case study. The cost of energy, renewable fraction, environmental impact, and breakeven grid extension distance are the main criteria that have been considered to determine the optimal size of PV/DG/B to supply the load demand. HOMER$^{®}$ software is used to perform the simulation and optimization. For this case study, the minimum cost of energy and the minimum total present cost are 0.074 \$/kWh and 207676 \$, respectively. This is achieved by using a RO-500 unit and a LF dispatch control strategy. The related sizes to the best option of PV/DG/B are 120 kW PV array, 10 kW DG, 64 batteries, and 50 kW converter. A comparison with grid extension and installing stand-alone diesel generation is also carried out. The results of comparison have confirmed that the grid connection is better than all considered options using the RO-250 unit. However, for the RO-500 unit, all options of hybrid PV/DG/B are more economically feasible compared with grid connection, and the best cost-effective option is the one including LF strategy with 10 kW DG. Stand-alone diesel generator produces 119110 kg/year and 117677 kg/year of CO$_2$ respectively for RO-250 and RO-500.

INDEX TERMS Energy management, energy efficiency, water pumping, desalination, hybrid system.

I. INTRODUCTION

Egypt's Vision 2030 depends on using renewable energy sources to minimize, or eliminate, the CO$_2$ emissions to reduce the effect of Global Warming [1]. Egypt is one of the largest producers of Oil in Africa outside of the OPEC (Organization of the Petroleum Exporting Countries) and the third large producer of Natural Gas. Also, the Suez Canal plays

The associate editor coordinating the review of this manuscript and approving it for publication was Sudhakar Babu Thanikanti .

the main role in the international energy market [1]. Egypt is one of the populous countries in the Middle East and faces energy demand due to rapid population growth and overcome our growing needs. This makes a great challenge to supply energy. Using renewable energy sources can help Egypt to achieve its demand for energy and create a lot of jobs with the achievement of objectives of sustainable development [2]. Global Warming is one of the biggest challenges that is facing humanity on Earth [3]. Harmful effects of using fossil fuels to generate electricity should be reduced, if not eliminated.
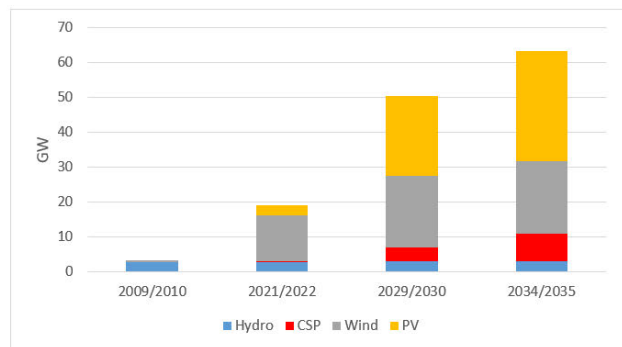
FIGURE 1. Generated renewable energy sources in Egypt, GW.

One of the important keys to solve the problems of Global Warming is to generate energy from renewable sources and improve its efficiencies [4]. Egypt is very rich with sources of renewable energy like hydropower, wind, solar PV, concentrating solar power (CPS), and biomass energy sources. The Egyptian government started programs of using renewable energy sources since the 1970s. It depends on its resources and also on co-operation with other countries, including Germany, France, Italy, Spain, Denmark, Japan, and the United States [5]. The Egyptian government focuses nowadays on using wind energy and solar photovoltaic (PV) applications, which include water pumping, cold stores, and desalination plants [5]. Figure 1 shows the generated renewable energy sources in Egypt up to 2035 in GW. The main planned PV projects in Egypt up to 2023, with its capacity and name of companies, are listed in Table 1 [5].

TABLE 1. Planned solar PV system projects in Egypt up to 2023.

Project name	Status	Capacity
Kom Ombo 1	Binding	200 MW
Kom Ombo 2	Under development	26 MW
Kom Ombo 3	Under development	50 MW
West Nile 1	Binding	600 MW
West Nile 2	Binding	200 MW
West Nile 3	Binding	600 MW
FIT 1	Operational	50 MW
FIT 2	Under development	1415 MW
Hurghada	Tendering	20 MW
Zaafarana	Under development	50 MW

Water desalination is the process of converting high salt-water to freshwater by removing salt particles. This water can be drinkable for humans or used for irrigation. Deferent desalination processes are used in industrial and commercial applications. With improvements in technology techniques, desalination processes are becoming cost-competitive and more efficient rather than other methods of producing fresh-water to overcome our growing needs [6]–[8]. However, the total cost of water desalination is still high by using conventional methods of energy source. So, the new trend now of Egypt's governments is using renewable energy systems, which will decrease the total cost to reasonable values, which will decrease the cost of energy compared with grid extension and diesel generation systems. In addition to the cost of treatment of environmental effects of using fossil fuel is so high for the long term; CO_2 emissions which an effect on Global Warming [9]–[12].

Using renewable energy systems for supplying desalination plants is increased. There are about 130 desalination plants around the world opened in the last few years [13]. Table 2 lists some of them with focusing on the name of desalination plant, its location, kind of technology if it is multi-effects distillation (MED) or reverse osmosis (RO), the capacity of the plant, and kind of renewable energy used.

TABLE 2. Selected renewable energy systems supplies desalination plants around the world.

Country	Desalination plant name	Desalination technology	Capacity (m³/day)	Renewable Energy Systems
Greece	Kimolos	MED	200	Geothermal
Japan	Keio University	MED	100	Solar Thermal
Spain	PSA	MED	72	Concentrating solar power (CSP)
Greece	Ydriada	RO	80	Wind turbine
Morocco	Morocco	RO	12-24	Solar PV cells
Scotland	Oyster	RO	n a	Wave energy

The energy management strategies (EMS) are the process of selecting, presenting, and programming a central-controller to manage the flow of energy according to an optimal-strategy. The central-controller can be a micro-controller, microprocessor, PLC, or any other type of suitable controller [14].

Several optimization programs and mathematical techniques are used to plan and design energy management strategies [15], which include stand-alone or Utility-connection systems, as concluded in Figure 2. HOMER®software
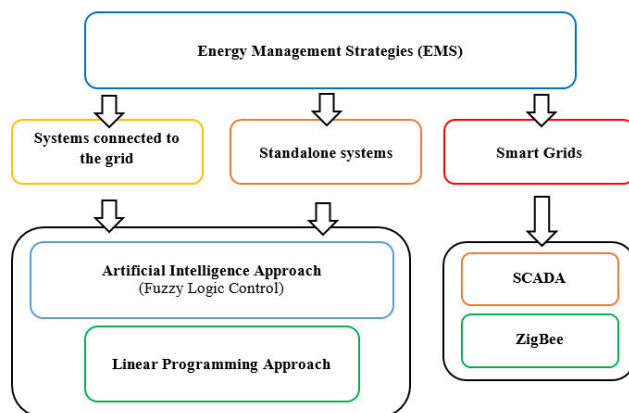

FIGURE 2. Energy management strategies (EMS) approaches commonly used.

TABLE 3. Summary of literature review.

Authors	Year	Hybrid Configuration	Control strategies
Bizon et al. [24]	2020	PV/Wind/ Fuel Cell	RTO: Air-LFW and Fuel-LFW
Rezk et al. [25]	2020	PV/FC/Battery	Linear programming
Krishan et al. [26]	2020	PV/Wind/Supercapacitor/Utility	OPAL-RT
Aziz et al. [27]	2019	PV/Hydro/DG/Battery	Linear programming
Aziz et al. [28]	2019	PV/DG/Battery	Linear programming
Zhou et al. [29]	2019	Wind/Biomass/DG/Battery	Parallel double-mode optimal operation strategy
Das et al. [15]	2017	PV/ Battery/ICE (DG)	Genetic Algorithm (GA)
Nasri et al. [30]	2016	PV/Fuel Cell/Ultra-Capacitor	Linear programming
Upadhyay et al. [31]	2016	PV/Wind/DG/Battery	PSO Genetic algorithm Biogeography
Athari et al. [32]	2016	PV/Wind/Battery/Utility	Fuzzy logic
Pascual et al. [33]	2015	PV/Wind/Battery/Utility	Linear programming
Barrazouane et al. [34]	2014	PV/DG/Battery	Cuckoo search algorithm Fuzzy logic controller
Karami et al. [35]	2014	PV/Battery/Super-Capacitor/Fuel Cell/Utility	Linear programming
Ismail et al. [36]	2013	PV/Battery/DG	Linear programming
Dahmane et al. [37]	2013	PV/Wind/DG/Battery	Linear programming
Feroldi et al. [38]	2013	PV/Wind/Bioethanol reformer	State machine approach
Chen et al. [39]	2013	PV/Wind/Battery	Fuzzy logic
Robyns et al. [40]	2013	PV/Wind/Battery/Utility	Fuzzy logic
Basnet et al. [41]	2020	PV/Hydrogen/Fuel cell/Grid	P2G Technology
Mayer et al. [42]	2020	PV/Wind/Grid/DG	Genetic Algorithm
Tutkun et al. [43]	2016	PV/Wind/Battery	Neural networks

is an optimizing program that can optimize several techniques [16], [17], which are used throughout many studies to investigate the optimal design of the proposed renewable energy system based on LF [18]–[20] or CC strategies [21]–[23]. Table 3 summarizes the literature review of renewable energy systems based on hybrid configuration and simulation tools of control strategies.

In this paper, the authors' contribution is to evaluate a proposed stand-alone PV/DG/B system that supplies a real load in Al-Minya city, Egypt. The used simulation tool is HOMER® software to get the optimal size and best energy management strategy for this case study. A comparison of the proposed system with grid extension and also with installing stand-alone diesel generation has been carried out. Using PV/DG/B can significantly minimize the amount of CO_2 emissions generated in the case of a stand-alone diesel system and helps to treat Global Warming. Also, this research work is aimed to help policymakers in Egypt, location of case study, to develop and integrate the effective policy for energy-water nexus and energy-water-food security by achieving strict and fast rules of renewable energy systems for freshwater production through desalination plants and agriculture purposes, respectively. Using renewable energy in desalination water will help the economy to grow and supply sustainable water sources.

II. LOCATION AND LOAD DATA

The case study represents a flat 70 acres (283280 m^2) located in Minya city, Egypt, at the latitude of 28° N and longitude of 30° E. The site under study is positioned 12 km far away from UG connection. Minia city is characterized by a good level of solar radiation. The average daily horizontal solar radiation is around 5.97 kWh/m^2. The mean daily solar radiation level and clearance index during the year are shown in Figure 3 [44]. The highest daily irradiance level of 8.056 kWh/m^2 is collected in June. Whereas the least daily irradiance level of 3.555 kWh/m^2 is received in December. Figure 4 shows the solar atlas of Egypt [45], which is a sun-belt and high solar radiation country. The duration of sunshine is about 9 to 11 hours per day all year except a few cloudy days.
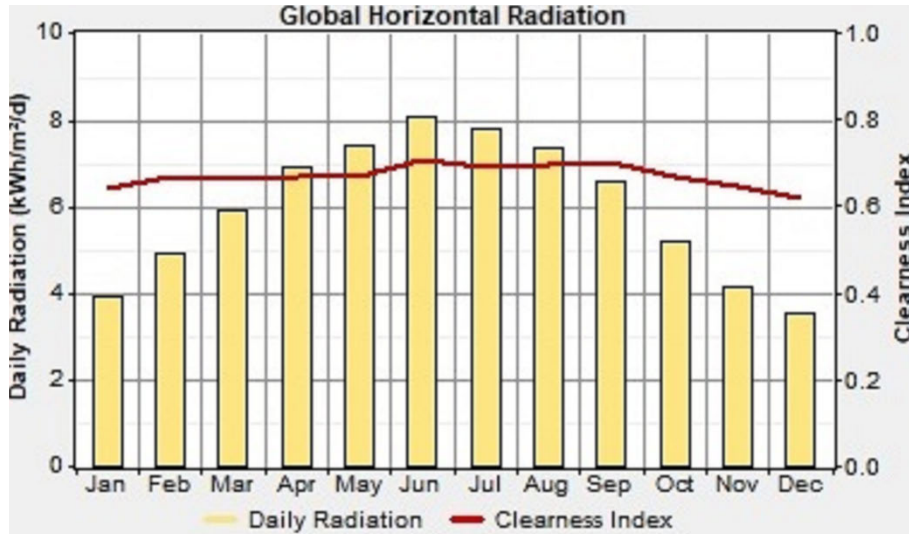
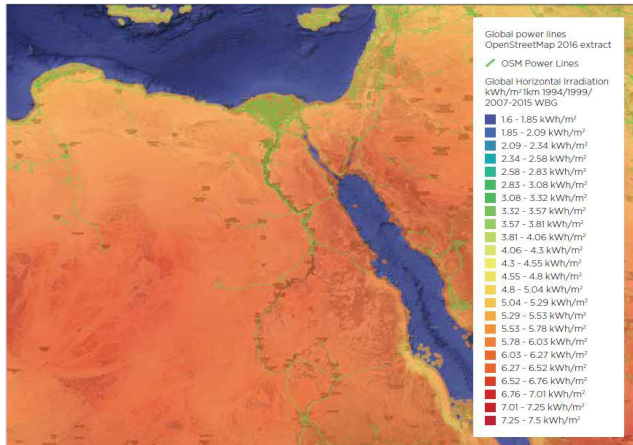**FIGURE 3.** Mean daily solar radiation level and clearance index during the year.

FIGURE 4. Solar atlas of Egypt (https://globalsolaratlas.info/).

In the location of the case study, there is a 150 m depth well with a 40 m static level of water, which produces 120 m^3 per hour of brackish water with a salinity of 2500 mg/l. It is planned to cultivate the land with some crops which can use the raw brackish water, whereas a large part of the land will be cultivated with other crops such as Wheat, which needs water with salinity less than 800 mg/l. The daily required desali- nated water is 250 m^3. The total brackish water demands are 350-500 m^3 and 250-300 m^3 of water in summer and winter seasons, respectively.

The electric power necessary to pump the required water can be estimated by the following relation [46], [47];

$$P_{pump} = \frac{2.725QH}{1000\eta} \qquad (1)$$

where P_{pump} denotes the power of the pump (kW); H denotes the water head of the pump (m), and η denotes the pump.

Based on the relation (1), the estimated daily electri- cal demand power to pump the water from well is around 110 kWh with a maximum of 15 kW. The seasonal load profile of the AC pump is illustrated in Figure 5-a. To desali- nate the brackish water, it is planned to use reverse osmo- sis (RO) desalination system. There are different sizes of RO units; 50 m^3, 100 m^3, 150 m^3, 250 m^3, 500 m^3, and 1000 m^3. The power consumption for each unit are 4.1 kW, 7.7 kW, 10.5 kW, 15 kW, 29.5 kW and 52 kW respec- tively for RO-50, RO-100, RO-150, RO-250, RO-500 and RO-1000 [48]. As the required desalinated water is 250 m^3, the three sizes, RO-50, RO-100, and RO-150, are not appli- cable to the study. The two sizes, RO-250 and RO-500, are compared in this research work to investigate and identify the economical option to desalinate the required quantity. RO-250 will operate 24 hours every day to get 250 m^3, whereas RO-500 needs only 12 hours to desalinate the same amount. It is planned to operate RO-500 from 6:00 AM to 6:00 PM. The seasonal load profiles of RO-500 and RO-250 are displayed in Figure 5-b and Figure 5-c, respectively. RO unit components' schematic diagram is shown in Figure 6.

III. MATHEMATICAL MODELING OF DIFFERENT COMPONENTS OF THE PROPOSED SYSTEM

Figure 7 shows a schematic diagram of the proposed renew- able energy system, which consists of solar PV cells, diesel generator, converter, and batteries. The input techno- economic parameters for all components in the proposed renewable energy system are listed in Table 4 [25], [49], [50], which is used to find the optimal sizes for the proposed system using HOMER® software [51], [52].

A. MODELLING OF SOLAR PV CELLS

The output power (P_{PV}) from solar PV cells at any time (t) is affected by several factors such as solar radiation (R), PV array area (A_{Array}), the efficiency of the converter (η_c), the efficiency of the PV cells (η_{PV}) and environmental factors
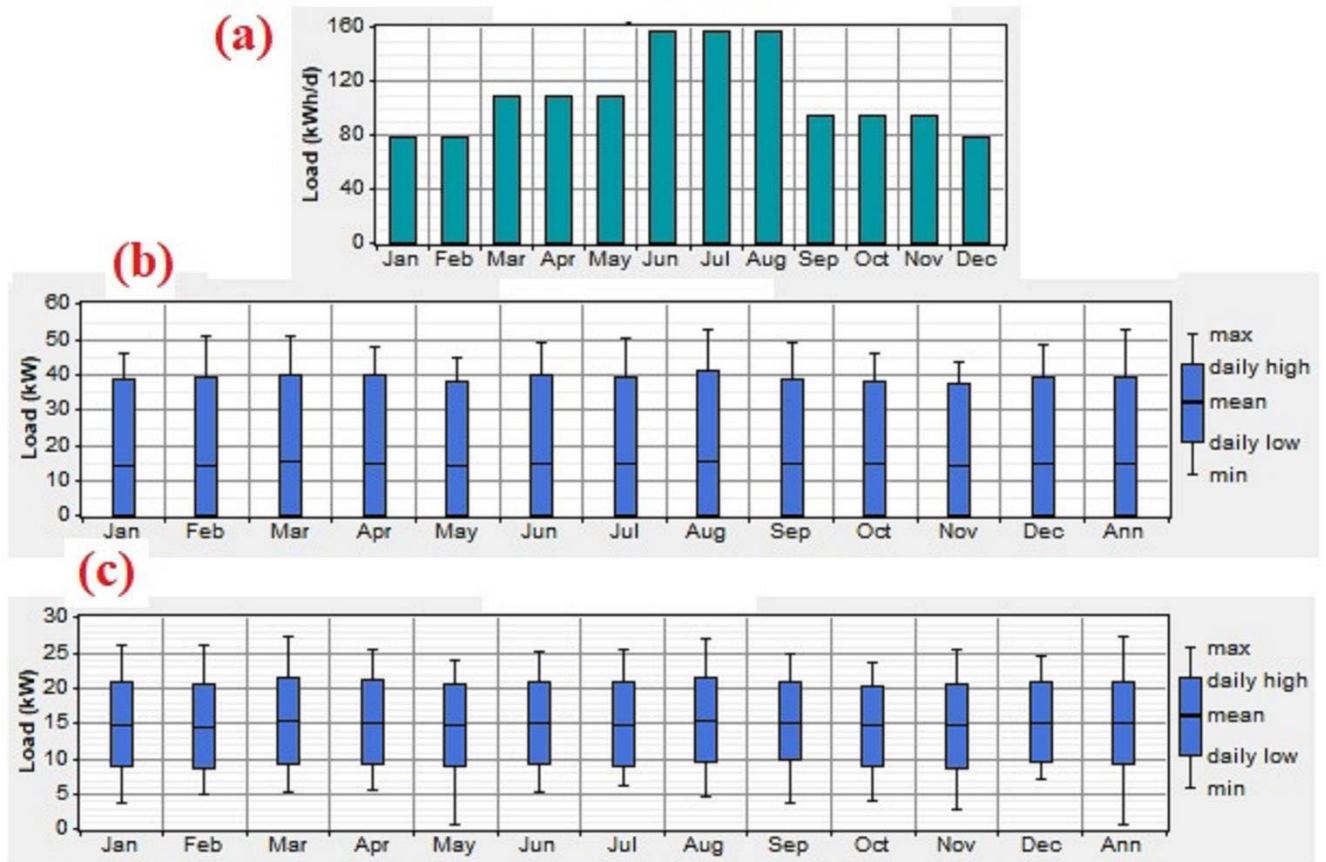
FIGURE 5. Seasonal load profile (a) AC water pump; (b) RO-500 unit; (c) RO-250 unit.
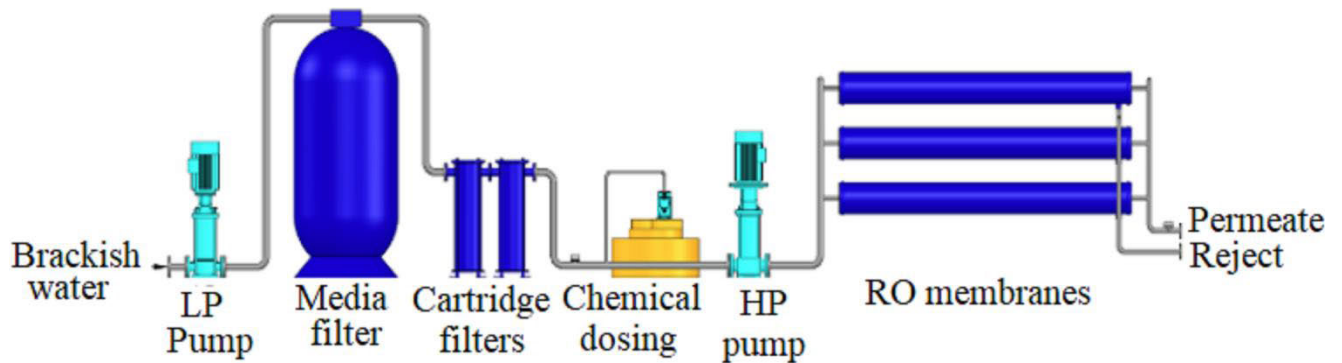

FIGURE 6. Schematic diagram of RO unit components.

such as ambient temperature, wind velocity [25], [53].

$$P_{PV} = R \times \eta_{PV} \times \eta_c \times A_{array} \quad (2)$$

The output of the PV cells is affected by the ambient temperature. So, the temperature of PV cell (T_c) depends on effective transmittance absorbance of the solar PV array (α), the coefficient of heat transfer (T_H) and the efficiency of the PV cells (η_{PV}) which are expressed as follows:
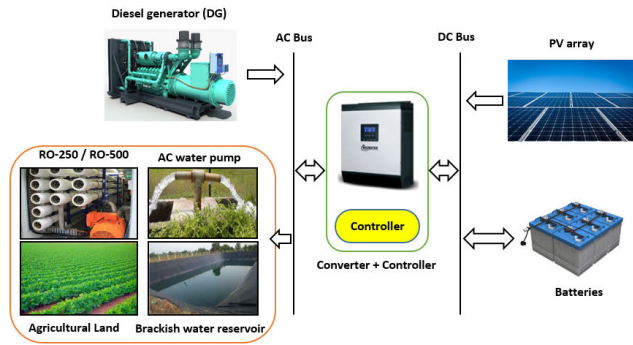
$$T_c = T_a + R.\left(\frac{\alpha}{T_H}\right)\left(1 - \frac{\eta_{PV}}{\alpha}\right) \quad (3)$$

The net present cost (NPC_{PV}) of the solar PV cells is calculated by using the capital cost (C_{PV}), operation, and maintenance ($C_{OM}.PV$) costs per year as expresses by the following equation:

$$NPC_{PV} = C_{PV} + C_{OM.PV} \quad (4)$$

$$C_{PV} = \eta_{PV}.A_{array} \quad (5)$$

$$C_{OM.PV} = A_{array}.\sum_{i=1}^{n}\left(\frac{1+\beta}{1+r}\right)^i \quad (6)$$

FIGURE 7. Schematic diagram of the proposed renewable energy system.

TABLE 4. Summary of proposed renewable energy system components.

Component	Specification
Solar PV cells	
Model name	Generic flat plate PV
Peak power	1 kW
Slop	28o
Ground reflection	27%
Operating temperature	46o
Efficiency	14.7%
Capital cost	$1000
Replacement cost	$1000
O&M cost	$5/year
Life time	25 years
Batteries (BS)	
Model name	Trojan L16P
Nominal capacity	360 Ah, 2.16 kWh
capital cost	175 $/one unit
cost of replacement	175 $/one unit
O&M cost	5 $/year
Converter	
Capital cost	500 $/kW
Replacement cost	450 $/kW
O&M cost	$5/year
Lifetime	15 years
Efficiency	90%
Diesel Generator (DG)	
Capital cost	230 $/kW
Replacement cost	230 $/kW
O&M cost	0.1 $/hour
fuel price	0.428$/L
Diesel generator lifetime	15000 h

where, (r) is the interest, and (β) is the escalation rates; these economic aspects have been considered in the optimization process.

B. MODELLING OF THE BATTERY SYSTEM

The authors have used lead-acid batteries in this study to store the excess energy generated from the solar PV cells and DG. The battery power (P_B) can be calculated by the following

equation [25], [53]:

$$Q_B = Q_{B-i} + \int_0^t V_B.I_B.dt \quad (7)$$

where Q_{B-i} is the initial battery charge; V_B and I_B are voltage and current rating of the battery, respectively. The battery state of charge (B_{SoC}) can be expressed as:

$$B_{SoC} = \frac{Q_B}{Q_{B-max}} \times 100\,(\%) \quad (8)$$

where Q_{B-max} is the maximum charge of the battery. The capacity of a battery (C_{Wh}) can be calculated from the following formula [25]:

$$C_{Wh} = (P_L \times A_d)/(\eta_C \times \eta_{BS} \times D_d) \quad (9)$$

where P_L: load demand energy, kWh/day; Ad: BS autonomy per day; D_d: discharge depth; η_{BS} and η_C are the efficiency of battery and converter, respectively.

C. MODELING OF DIESEL GENERATOR

The electrical power output (P_{DG}) from the diesel generator is AC power and depend on the fuel consumption from the DG. The fuel curve assumed a straight line in HOMER modeling for simplicity. Rate of fuel consumption (F) is calculated for electricity production [50]:

$$F = A_1.C_{DG} + A_2.P_{DG} \quad (10)$$

where; A_1 is coefficient of the fuel curve, A_2 is the slope of fuel curve, which its values are obtained from the manufacturer's datasheet which equal to 0.246 L/kWh and 0.08145 L/kWh, respectively, C_{DG} is the diesel generator capacity, and P_{DG} is the electrical power output from DG. This equation can be applied when the DG is running, while the DG is at rest, the fuel consumption rate (F) is zero. The replacement cost of DG is calculated to depend on the number of operating hours.

The net present cost of diesel generator (NPC_{DG}) depends on the capital cost of the diesel generator (C_{DG}), fuel cost (F), operating and maintenance cost (C_{OM-DG}) and the cost of the replacement (C_{R-DG}) as expressed by the following equation:

$$NPC_{DG} = C_{DG} + C_{OM-DG} + C_{R-DG} + F \quad (11)$$

$$C_{DG} = \eta_{DG}.P_{DG} \quad (12)$$

$$C_{OM-DG} = t_{run}.\sum_{i=1}^{n}\left(\frac{1+\beta}{1+r}\right)^i \quad (13)$$

IV. ENERGY MANAGEMENT STRATEGIES

To determine the energy flows, the controller compares the generated power value (P_{PV}) of Solar PV cells with the load demand (P_L). If the renewable energy from solar PV cells (P_{PV}) greater than load demand (P_L), the excess power goes to charge the batteries if its state of charge level is not reaching its maximum value (B_{Soc_max}). If the load demand (P_L) is lower than the renewable power (P_{PV}) and state of charge of batteries not reach its minimum value (B_{Soc_min}), batteries
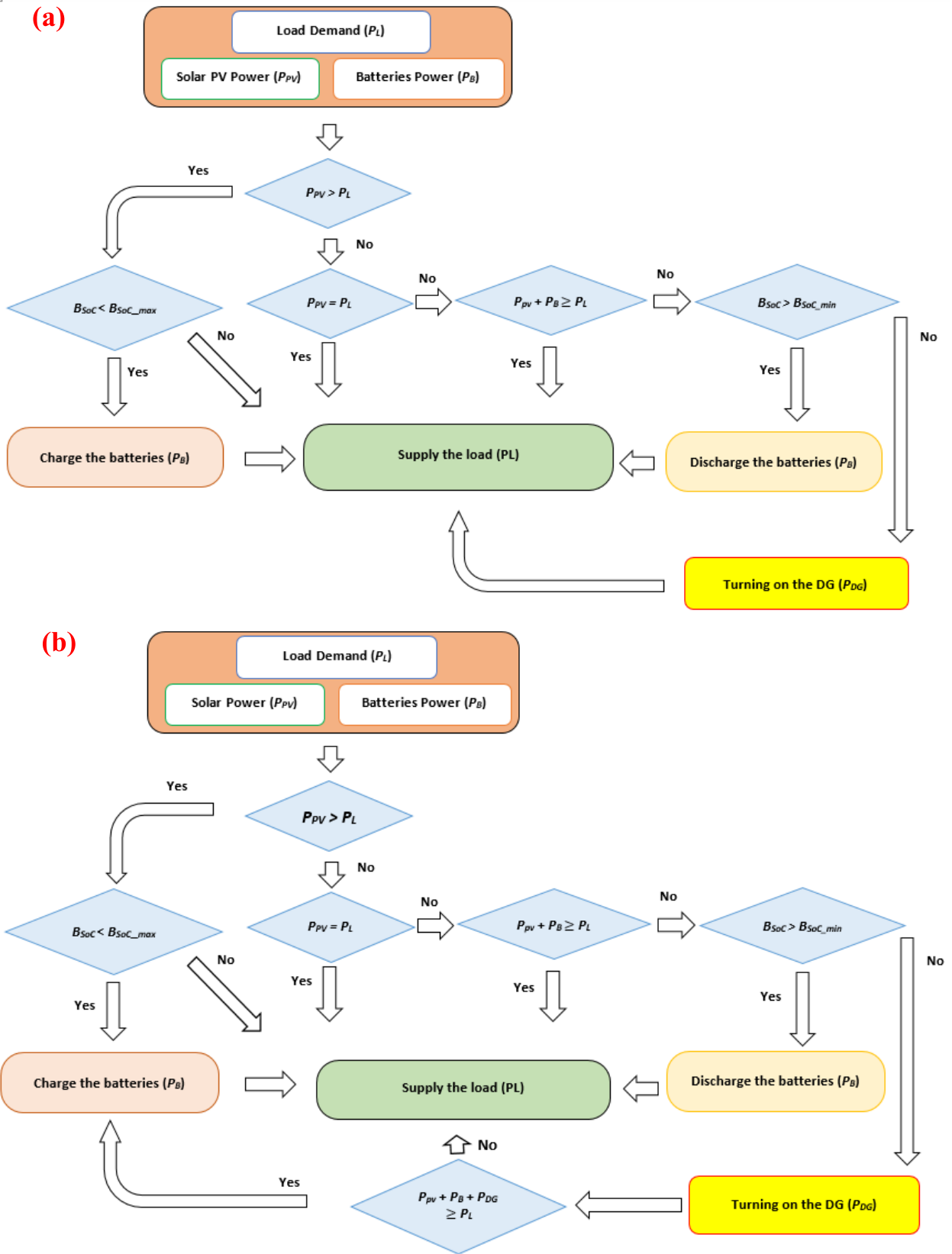
(a)

(b)

FIGURE 8. Power management strategies (PMS) to supply the load; (a) Load following (LF) and (b) Cycle charging (CC) Strategies.

TABLE 5. The optimal size of PV/DG/BS system and related costs with varying size of RO, control strategy and size of DG.

|	PV (kW)	DG (kW)	No of Batteries	Converter (kW)	Operating cost ($/yr.)	Renewable Fraction	Initial cost ($)	NPC ($)	COE ($/kWh)
					RO-250				
Only DG	-	25	-	-	27155	0.0	6250	604298	0.164
PV-B	120	-	384	35	13994	1.0	204316	512505	0.138
				PV-B-DG - Load Following Control Strategy					
DG, 5 kW	90	5	320	30	13295	0.87	161930	454729	0.123
DG, 10 kW	75	10	160	35	12737	0.75	122840	403356	0.109
				PV-B-DG – Cycle Charging Control Strategy					
DG, 5 kW	95	5	224	30	14875	0.84	150226	477812	0.129
DG, 10 kW	70	10	96	30	15664	0.67	104204	449181	0.121
					RO-500				
Only DG	-	45	-	-	28134	0.0	11250	630856	0.171
PV-B	120	-	160	35	5445	1.0	175340	295252	0.081
				PV-B-DG - Load Following Control Strategy					
DG, 5 kW	110	5	128	55	5546	0.97	161022	283168	0.077
DG, 10 kW	120	10	64	50	5087	0.95	158636	270676	0.074
				PV-B-DG – Cycle Charging Control Strategy					
DG, 5 kW	115	5	64	50	9549	0.88	152386	362691	0.099
DG, 10 kW	105	10	32	45	11774	0.81	135568	394873	0.108
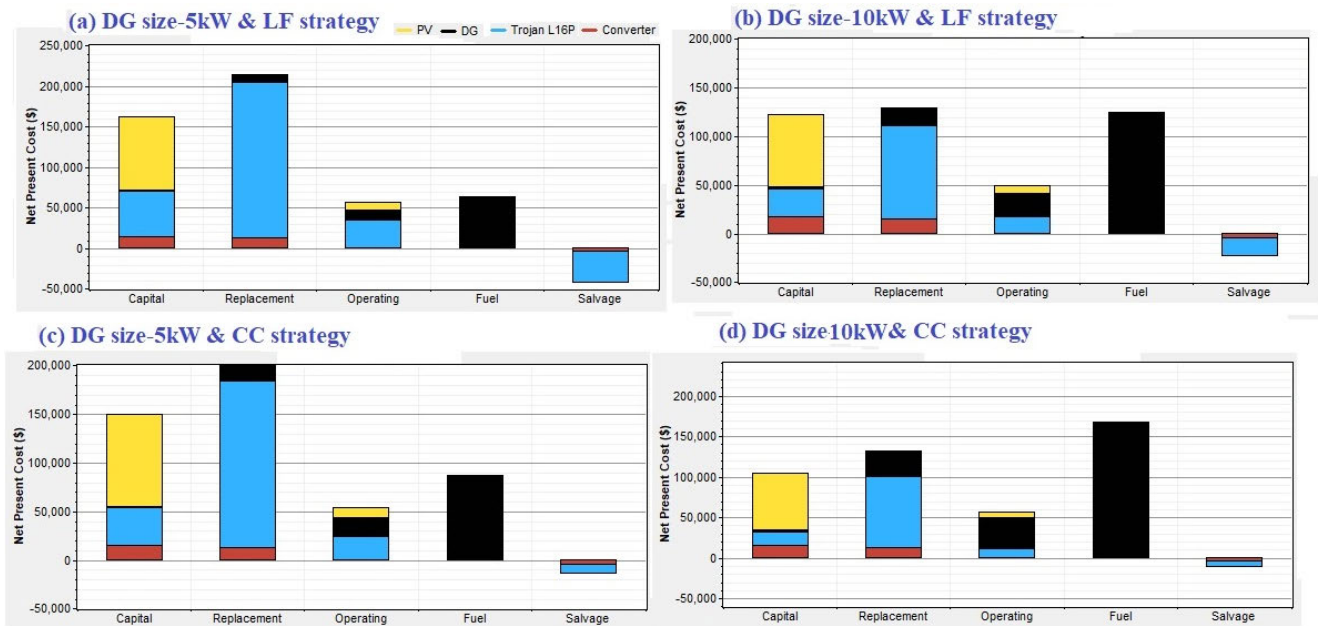
FIGURE 9. The total NPC for different system components with RO-250 unit.

can discharge its power (P_B) supplies to the load. If the state of charge of batteries reaches its minimum value (B_{Soc_min}), here the DG must start-up, and its power (P_{DG}) supplies the load.

Figure 8 shows the Power Management Strategies (PMS), which include two control dispatch strategies; load following (LF) and cycle charging (CC). These dispatch strategies are used to control DG operation and battery. With the LF strategy, a DG generates only sufficient energy to meet the required load and does not charge the battery bank. The battery bank is charged only by surplus power by PV arrays

Figure 8-a. With the CC strategy, the DG works at its maximum rating whenever it is switched on to supply load and charge the battery bank by the surplus energy, Figure 8-b.

V. OPTIMIZATION PROBLEM FORMULATION

The optimum size of PV/DG/B has been determined based on the minimum total net present cost (NPC) and the minimum cost of energy (COE). The NPC can be estimated based on the following relation;
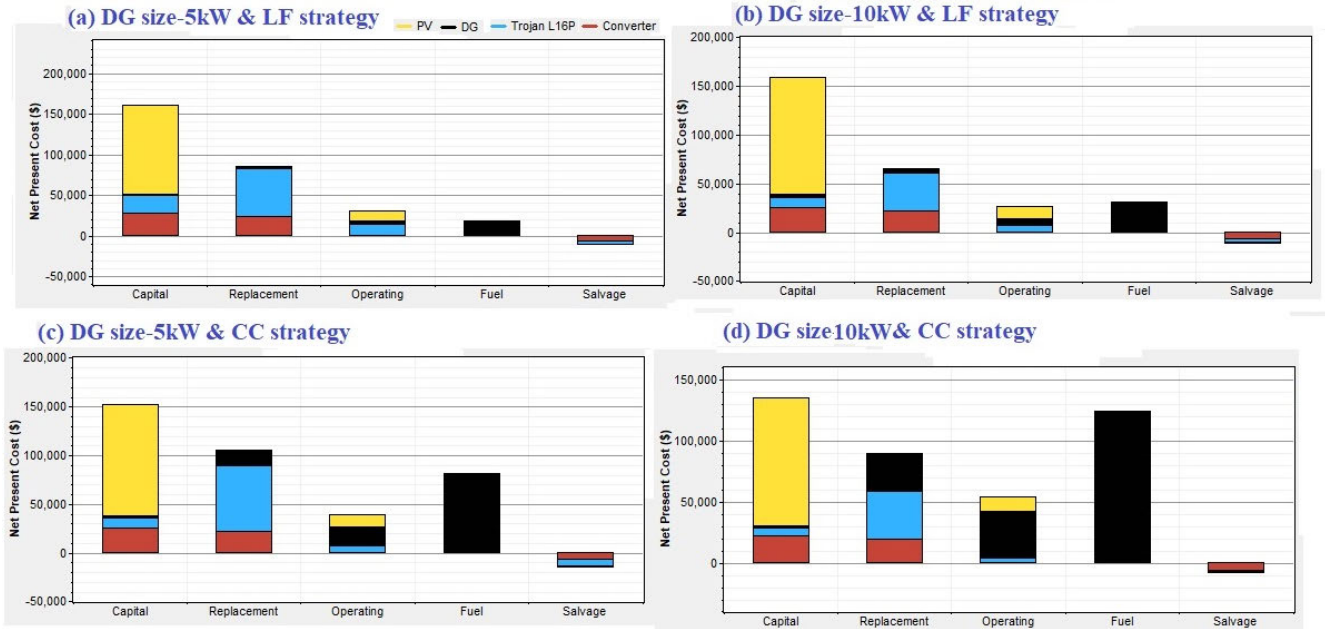
$$NPC = \frac{C_{ann,tot}}{CRF_{(i,N)}}, \qquad (14)$$

FIGURE 10. The total NPC for different system components with RO-500 unit.

TABLE 6. Related costs of different components for PV/DG/B system using RO-250.

	Capital ($)	Replacement ($)	O&M ($)	Fuel ($)	Salvage ($)	Total ($)
		Load Following Control Strategy				
		Size of DG - 5kW				
PV array	90,000	0	9,910	0	0	99,910
DG	1,250	8,831	11,703	63,814	-140	85,459
Battery	55,680	192,044	35,237	0	-37,623	245,338
Converter	15,000	12,920	0	0	-3,899	24,021
System	161,930	213,795	56,851	63,814	-41,661	454,729
		Size of DG - 10kW				
PV array	75,000	0	8,259	0	0	83,259
DG	2,500	17,656	23,345	124,827	-325	168,003
Battery	27,840	96,209	17,619	0	-17,598	124,069
Converter	17,500	15,074	0	0	-4,549	28,025
System	122,840	128,939	49,222	124,827	-22,472	403,356
		Cycle Charging Control Strategy				
		Size of DG - 5kW				
PV array	95,000	0	10,461	0	0	105,461
DG	1,250	15,437	19,292	87,070	-390	122,659
Battery	38,976	171,275	24,666	0	-9,246	225,671
Converter	15,000	12,920	0	0	-3,899	24,021
System	150,226	199,632	54,419	87,070	-13,535	477,812
		Size of DG - 10kW				
PV array	70,000	0	7,708	0	0	77,708
DG	2,500	30,874	38,585	167,737	-780	238,916
battery	16,704	87,838	10,571	0	-6,578	108,535
Converter	15,000	12,920	0	0	-3,899	24,021
System	104,204	131,632	56,864	167,737	-11,257	449,181

where $C_{ann,tot}$ denotes total cost per year, i denotes yearly real interest rate, N is project lifetime years), and CRF denotes the capital recovery factor. CRF is calculated as follows;

$$CRF(i, N) = \frac{i(1 + i)^N}{(1 + i) - 1}. \quad (15)$$

The total cost $C_{ann,tot}$ includes initial cost, operation, maintenance, and replacement. The salvage value can be estimated by the following relation:

$$Salvage = C_{rep}\frac{R_{rem}}{R_{comp}}, \quad (16)$$

where:

C_{rep} is the replacement cost of the components,

R_{rem} is the remaining life,

and R_{comp} is the project life span.

The COE can be calculated as follows:

$$COE = \frac{C_{ann,tot}}{Total\ energy\ demand}, \quad (17)$$

VI. RESULTS AND DISCUSSION

This section presents the detailed feasibility and techno-economic evaluation of the PV/DG/B system to supply the

TABLE 7. Related costs of different components for PV/DG/B system using RO-500.

|	Capital ($)	Replacement ($)	O&M ($)	Fuel ($)	Salvage ($)	Total ($)
			Load Following Control Strategy			
			Size of DG - 5kW			
PV array	110,000	0	12,113	0	0	122,113
DG	1,250	2,177	3,537	18,509	-315	25,158
Battery	22,272	58,727	14,095	0	-3,236	91,858
Converter	27,500	23,687	0	0	-7,148	44,039
System	161,022	84,591	29,744	18,509	-10,699	283,168
			Size of DG - 10kW			
PV array	120,000	0	13,214	0	0	133,214
DG	2,500	4,284	6,325	31,344	-1,183	43,271
Battery	11,136	39,035	7,047	0	-3,062	54,156
Converter	25,000	21,534	0	0	-6,498	40,036
System	158,636	64,852	26,586	31,344	-10,743	270,677
			Cycle Charging Control Strategy			
			Size of DG - 5kW			
PV array	115,000	0	12,663	0	0	127,663
DG	1,250	15,433	19,253	80,818	-419	116,334
Battery	11,136	67,972	7,047	0	-7,498	78,657
Converter	25,000	21,534	0	0	-6,498	40,036
System	152,386	104,939	38,963	80,818	-14,415	362,691
			Size of DG - 10kW			
PV array	105,000	0	11,562	0	0	116,562
DG	2,500	30,870	38,545	123,932	-809	195,038
battery	5,568	39,273	3,524	0	-1,124	47,241
Converter	22,500	19,380	0	0	-5,848	36,032
System	135,568	89,524	53,631	123,932	-7,781	394,873
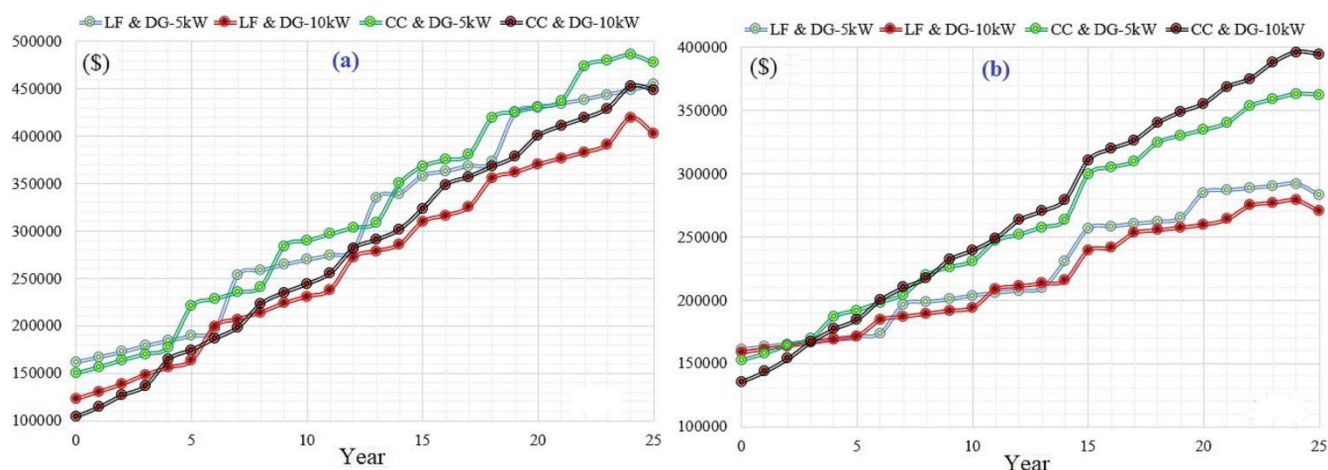
FIGURE 11. The discounted cash flows of the PV/DG/B system with varying; (a) RO-250; (b) RO-500.

AC pump and RO unit. To identify the cost-effective and best size of PV/DG/B system, two different sizes of RO units; RO-250 and RO-500, two control dispatch; LF and CC; two sizes of DG; 5 kW and 10 kW are considered in the case study. Four main criteria; the cost of energy, renewable fraction, environmental impact, and breakeven grid extension distance are used to identify the optimal size of PV/DG/B to supply the load demand.

From the economic point of view, the cost of energy varies from 0.108 $/kWh-0.074 $/kWh and from

TABLE 8. Electrical energy production and consumption.

| Item	Component	RO-250			
		Load Following Control Strategy Size of DG-5 kW	10 kW	Cycle Charging Control Strategy Size of DG-5 kW	10 kW
Electrical production (kWh/yr.)	PV	180398 (87%)	150324 (75%)	190410 (84%)	140302 (67%)
	DG	26221 (13%)	51232 (25%)	35344 (16%)	67905 (33%)
	Total	206610 (100%)	201556 (100%)	225754 (100 %)	208207 (100%)
Consumption energy (kWh/yr.)	RO-250	128431 (76%)	129001 (77%)	128362 (76%)	128829 (76%)
	AC Pump	39536 (24%)	39067 (23%)	40017 (24%)	39723 (24%)
	total	167967 (100%)	168068 (100%)	168397 (100%)	168553 (100%)
Excess electricity	(KWh/yr.)	14209 (6.88%)	16101 (7.99%)	34048 (15.1%)	24145 (11.6%)
Unmet load	(KWh/yr.)	2903 (1.7%)	2770 (1.62%)	2486 (1.5%)	2319 (1.4%)
Capacity shortage	(KWh/yr.)	3451 (2.02%)	3436 (2.01 %)	2992 (1.8%)	3033 (١,٨%)
		RO-500			
Electrical production (kWh/yr.)		Load Following Control Strategy Size of DG-5 kW	10 kW	Cycle Charging Control Strategy Size of DG-5 kW	10 kW
	PV	220475 (97%)	240518(95%)	230497 (88%)	210453 (81%)
	DG	7587 (3%)	12804(5%)	32632 (12%)	48866 (19%)
	Total	228062 (100%)	253322(100%)	263129 (100%)	259319 (100%)
Consumption energy (kWh/yr.)	RO-500	126313 (76%)	126511(76%)	127330 (77%)	126553 (76%)
	AC Pump	39920 (24%)	40080 (24%)	38726 (23%)	40222 (24%)
	Total	166233 (100%)	166591 (100%)	166056 (100%)	166774 (100%)
Excess electricity	(KWh/yr.)	40998 (18%)	67671 (26.7%)	74813 (28.5%)	75695 (29.2 %)
Unmet load	(KWh/yr.)	2371 (1.4%)	2024 (1.2%)	2599 (1.5%)	1927 (1.1%)
Capacity shortage	(KWh/yr.)	3505 (2.1%)	3218 (1.9%)	3181 (1.9%)	3529 (2.1 %)
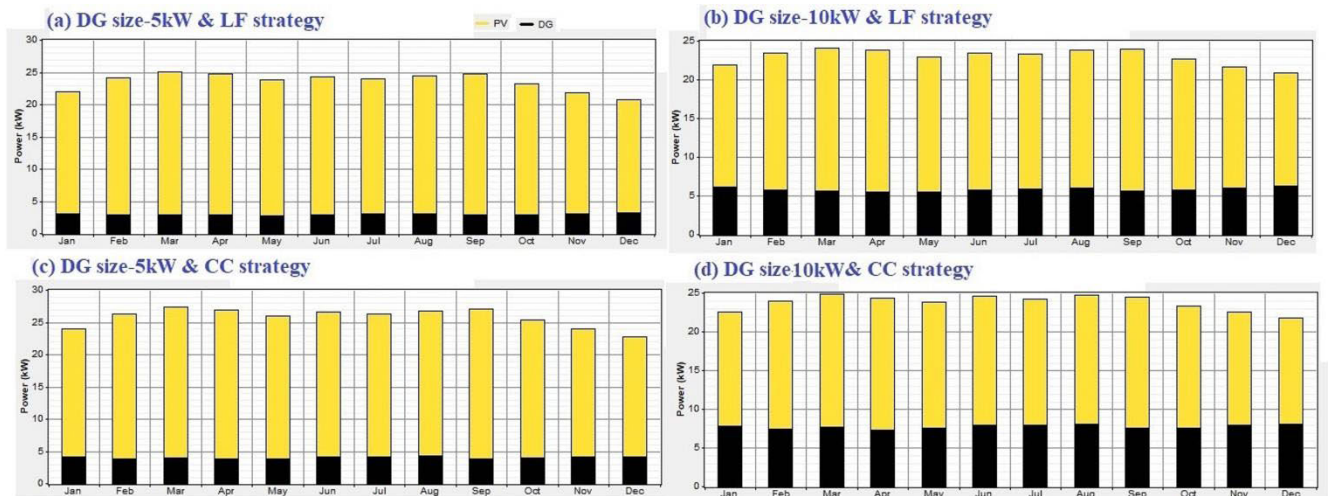
FIGURE 12. Mean produced electrical power with RO-250 unit varying control strategy and size of DG.

0.138 $/kWh-0.109 $/kWh respectively for RO-500 and RO-250. This demonstrates that using RO-500 is cost-effective compared with RO-250. The minimum cost of energy and the minimum total present cost are 0.074 $/kWh and 207676 $, respectively. This is achieved with RO-500 using load following dispatch control strategy. The related sizes to the optimal configuration are 120 kW PV array, 10 kW DG, 64 batteries, and 50 kW converter. The optimal size and related costs with varying sizes of RO,

control strategy, and size of DG are shown in Table 5. Using the LF strategy decreases the cost of energy with RO-500 by 22.2% and 31.48%, respectively, for DG size of 5kW and 10 kW compared with the CC control strategy.

Table 6 and Table 7 display the detailed related costs of different components for the PV/DG/B system for RO-250 and RO-500, respectively, with varying the control strategy and the size of DG. Whereas the total NPC for different system

TABLE 9. The detailed performance of different components of PV/DG/B system using RO-250 with varying control strategy and size of DG.

| Quantity	units	DG only	PV/B	LF Strategy		CC Strategy	
				DG-5 kW	DG-10 kW	DG-5 kW	DG-10 kW
PV array							
Rated capacity	kW	-	120	90	75	95	70
Mean output	kW	-	27	20.6	17.2	21.7	16
Daily mean output	kWh	-	659	494	412	522	384
Capacity factor	%	-	22.9	22.9	22.9	22.9	22.9
Total production	kWh/yr.	-	240518	180389	150324	190410	140302
Maximum output	kW	-	123	92.2	76.8	97.3	71.7
PV penetration	%	-	184	138	115	146	107
Levelized cost	$/kWh	-	0.0251	0.0251	0. 0251	0.0251	0.0251
DG							
Hours of operation	hr./yr.	8760	-	5314	5300	8760	8760
Number of starts	Starts/yr.	1	-	402	403	1	1
Operation life	yr.	1.71	-	2.82	2.83	1.71	1.71
Capacity factor	%	78.9	-	59.9	58.5	80.7	77.5
Total production	kWh/yr.	172818	-	26221	51232	35344	67905
Mean electrical output	kW	19.7	-	4.93	9.67	4.03	7.75
Min. electrical output	kW	2.83	-	0.05	0.1	0.05	0.1
Max. electrical output	kW	25	-	5	10	5	10
Fuel consumption	L/yr.	45232	-	6770	13243	9237	17795
Specific fuel consumption	L/kWh	0.262	-	0.258	0.258	0.261	0.262
Fuel electrical input	KWh/yr.	445080	-	66618	130311	90895	175106
Mean electrical efficiency	%	38.8	-	39.4	39.3	38.9	38.8
Battery							
Number of strings		-	12	10	5	7	3
Nominal capacity	kWh	-	829	691	346	484	207
Usable nominal capacity	kWh	-	581	484	242	339	145
autonomy	hr.	-	29.8	24.8	12.4	17.4	7.44
Lifetime throughout	kWh	-	412800	344000	172000	240800	103200
Energy in	kWh/yr.	-	90687	61121	30977	59121	28918
Energy output	kWh/yr.	-	77580	52737	26573	50580	24719
Losses	kWh/yr.	-	12612	8200	4162	8215	4062
Expected life	yr.	-	4.91	6.05	5.97	4.39	3.85
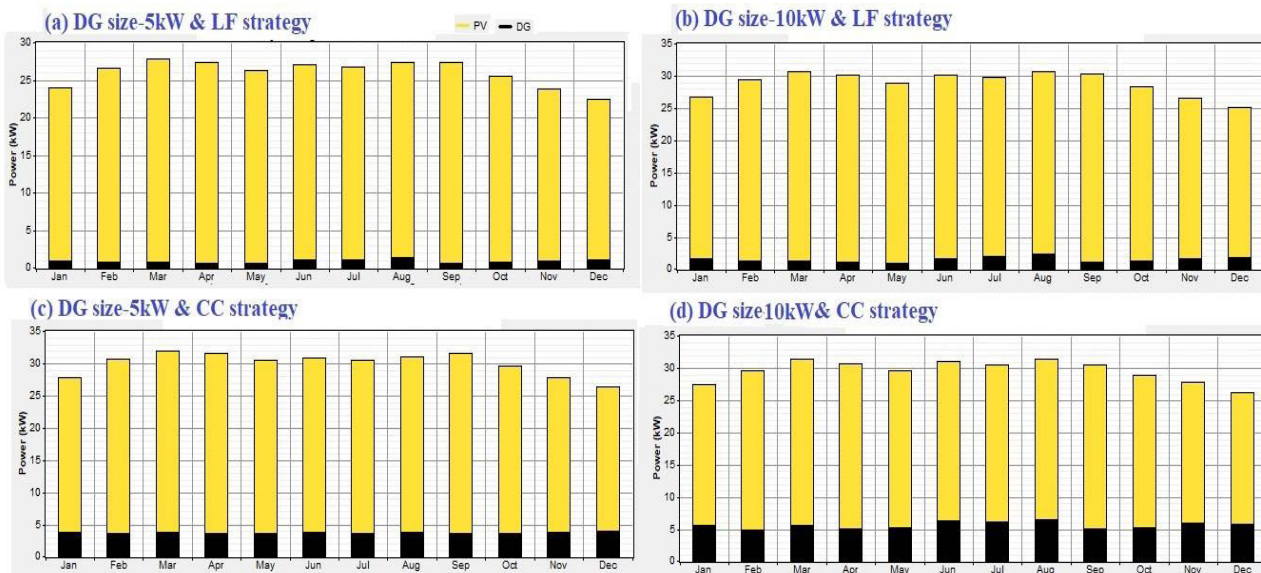
FIGURE 13. Mean produced electrical power with RO-500 unit varying control strategy and size of DG.

components is shown in Figure 9 and Figure 10, respectively, for RO-250 and RO-500. For RO-250 with 5 kW DG and LF strategy, the total NPC is 454729$. The replacement cost is 213795$ (47%) that represents the main part of the total NPC flowed by the initial cost (13.62%). The key reason for the high replacement cost is that the batteries need to be changed

TABLE 10. The detailed performance of different components of the PV/DG/B system using RO-500 with varying control strategy and size of DG.

Quantity	units	DG only	PV/B	PV/B/DG LF Strategy DG-5 kW	PV/B/DG LF Strategy DG-10 kW	PV/B/DG CC Strategy DG-5 kW	PV/B/DG CC Strategy DG-10 kW
PV array							
Rated capacity	kW	-	120	110	120	115	120
Mean output	kW	-	27	25	27	26	27
Daily mean output	kWh	-	659	604	659	631	659
Capacity factor	%	-	22.9	22.9	22.9	22.9	22.9
Total production	kWh/yr.	-	240518	220475	240518	230497	240518
Maximum output	kW	-	123	113	123	118	123
PV penetration	%	-	187	172	187	179	187
Levelized cost	$/kWh	-	0.0251	0.0251	0. 0251	0.0251	0.0251
DG							
Hours of operation	hr./yr.	5721	-	1606	1436	8742	8751
Number of starts	Starts/yr.	1458	-	907	898	2	2
Operation life	yr.	2.62	-	9.34	10.4	1.72	1.71
Capacity factor	%	42.7	-	17.3	14.6	74.5	55.8
Total production	kWh/yr.	168379	-	7587	12804	32632	48866
Mean electrical output	kW	29.4	-	4.72	8.92	3.73	5.58
Min. electrical output	kW	7.98	-	0.05	0.1	0.05	0.1
Max. electrical output	kW	45	-	5	10	5	10
Fuel consumption	L/yr.	44688	-	1964	3325	8574	13148
Specific fuel consumption	L/kWh	0.262	-	0.259	0.26	0.263	0.269
Fuel electrical input	kWh/yr.	439726	-	19323	32721	84368	129376
Mean electrical efficiency	%	38.3	-	39.3	39.1	38.7	37.8
Battery							
Number of strings		-	5	4	2	2	1
Nominal capacity	kWh	-	346	276	138	138	69.1
Usable nominal capacity	kWh	-	242	194	96.8	96.8	48.4
Autonomy	hr.	-	12.6	10.1	5.03	5.03	2.51
Lifetime throughout	kWh	-	172000	137600	68800	68800	34400
Energy in	kWh/yr.	-	29201	22540	13764	21241	13003
Energy output	kWh/yr.	-	25207	19352	11791	18107	11089
Losses	kWh/yr.	-	3969	2994	1880	3082	1878
Expected life	yr.	-	6.34	6.56	5.38	3.5	2.86

many times throughout the project lifetime. The replacement cost of batteries is 192044$, which represents 89.75% of the total replacement cost. Whereas with 10 kW, approximately, the capital, replacement, and fuel costs are very near. They are 122840$, 128939$, and 124827$, respectively, for capital, replacement, and fuel costs. The fuel cost records the maximum value of 167737$ with 10 kW of DG and CC strategy. It increased by 92.65% compared with 5 kW of DG and CC strategy. Considering Figure 10-b and Figure 10-d, it can be seen that the cost of fuel is mainly influenced by the dispatch control strategy. It is equal to 123932 $ and 31344$, respectively, for CC and LF strategies with the same size of DG (10 kW). This means that the cost of fuel reduced in the case of LF by 74.71% compared with the CC strategy.

The discounted cash flows related to PV/DG/B system with varying size of RO, control strategy, and size of DG is displayed in Figure 11. As explained in Figure 11-a, the lowest initial cost (104204$) is achieved with RO-250, CC strategy, and 10 kW size of DG. However, due to the high fuel cost (167737$) during the lifetime of the project, the total NPC has reached to 449181 $. The minimum total NPC of 403356 $ is achieved by using the load following strategy and 10 kW size of DG. Figure 11-b illustrates the variation of NPC using the RO-500 unit. It is clear from this figure that the maximum and

minimum total NPC are 394873 $ and 270676 $ respectively for CC and LF control strategies with the same size of DG (10 kW).

Under the condition of using the best size of the PV/DG/B system (RO-500, LF strategy, and 10 kW DG), the total yearly generated energy is 253322 kWh. 95% (240518 kWh) of the total produced energy is delivered by the PV system, and the reminder part (12804 kWh) is powered by DG. With this configuration, the total yearly consumption energy is 166591 kWh. The AC load pump consumed around 24% (40080 kWh) of the total consumed energy, while the other portion, 76% (126511 kWh), is used to feed the RO-500 unit. The surplus energy is almost 67671 kWh (26.7%). This surplus can be used for lighting and other not considered loads, whereas the annual unmet load and capacity shortage are 2024 kWh (1.2%) and 3218 kWh (1.9%), respectively. From Table 8, the annual excess energy is very sensitive to the size of RO. The minimum annual excess energy achieved with RO-250 unit, LF strategy, and 5 kW DG. Table 9 and Table 10 illustrate the detailed performance of different components of PV/DG/B systems with varying size of RO, control strategy and size of DG.

For RO-250, the rated capacities of the PV array are 90 kW, 75 kW, 95 kW, and 70 kW respectively for LF&5kW-DG,
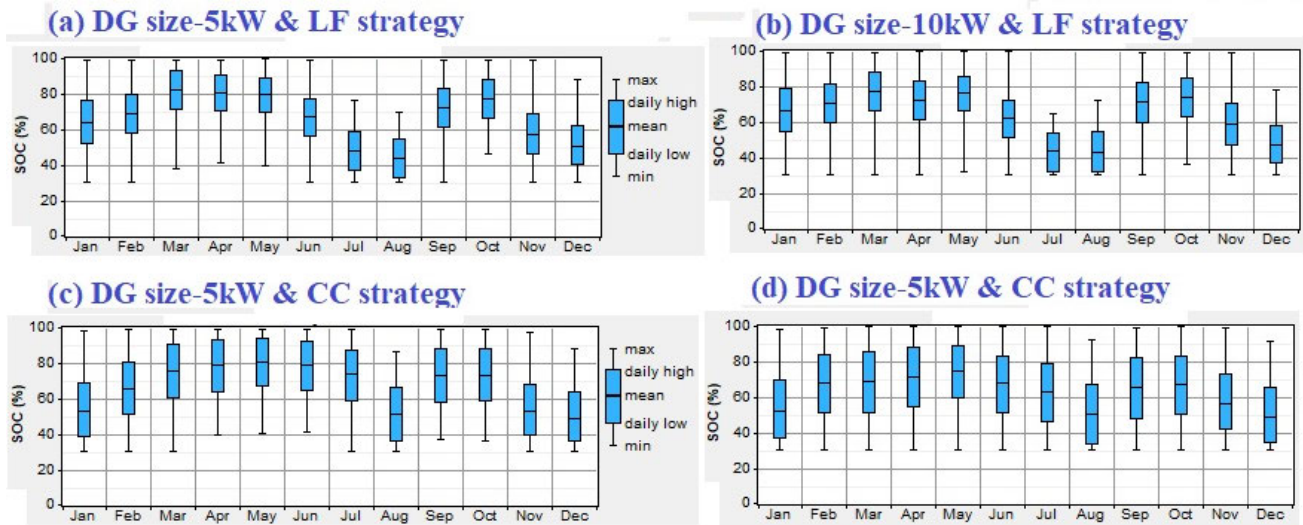
FIGURE 14. Statistics of battery SOC per month with RO-250 unit varying control strategy and size of DG.
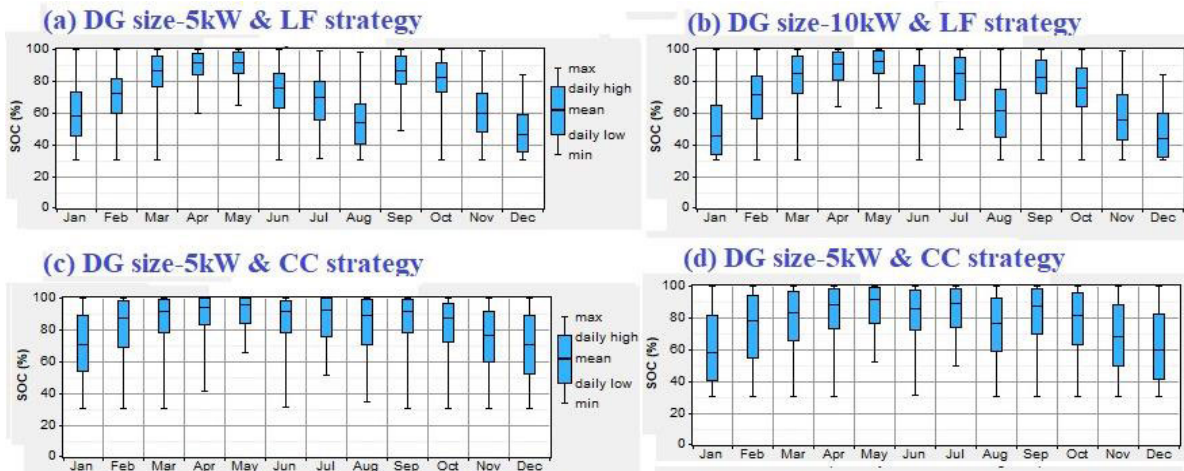

FIGURE 15. Statistics of battery SOC per month with RO-500 unit varying control strategy and size of DG.

LF&10kW-DG, CC&5kW-DG, and CC&10kW-DG. Subsequently, the mean PV output energy is 494 kWh, 412 kWh, 522 kWh, and 384 kWh, respectively, LF&5kW-DG, LF&10kW-DG, CC&5kW-DG, and CC&10kW-DG. The mean daily produced PV power for each month with varying control strategy and the size of DG is illustrated in Figure 12 and Figure 13, respectively, for RO-250 and RO-500.

For RO-500, the nominal capacities of battery are 276 kWh, 138 kWh, 138 kWh, and 69.1 kWh respectively for LF&5kW-DG, LF&10kW-DG, CC&5kW-DG, and CC&10kW-DG. Whereas the values of the expected life of the battery are 6.56 years, 5.38 years, 3.5 years, and 2.86 years respectively, LF&5kW-DG, LF&10kW-DG, CC&5kW-DG, and CC&10kW-DG. This is confirmed that the expected life of the battery is mainly influenced by the type of control strategy. The LF strategy increases the battery lifetime compared with the CC. The monthly statistics of battery SOC are presented in Figure 14 and Figure 15, respectively, for RO-250 and RO-500.

VII. COMPARISON WITH GRID EXTENSION AND STAND-ALONE DIESEL GENERATOR

To prove the viability of the PV/FC/B system, a comparison with grid extension along with a stand-alone diesel generator has been made. The initial cost of grid connection and yearly maintenance costs are $10,000/km and $200/year/km, respectively. The Energy consumption tariff, based on the Egyptian Electricity Company, is $0.06/kWh [54]. Figure 16 illustrates a comparison among the NPC of PV/DG/B with different conditions and NPC of the grid. Figure 17 displays a comparison of the breakeven grid extension distance with varying the RO size, control strategy, and size of DG. The red line represents the distance between the location of the
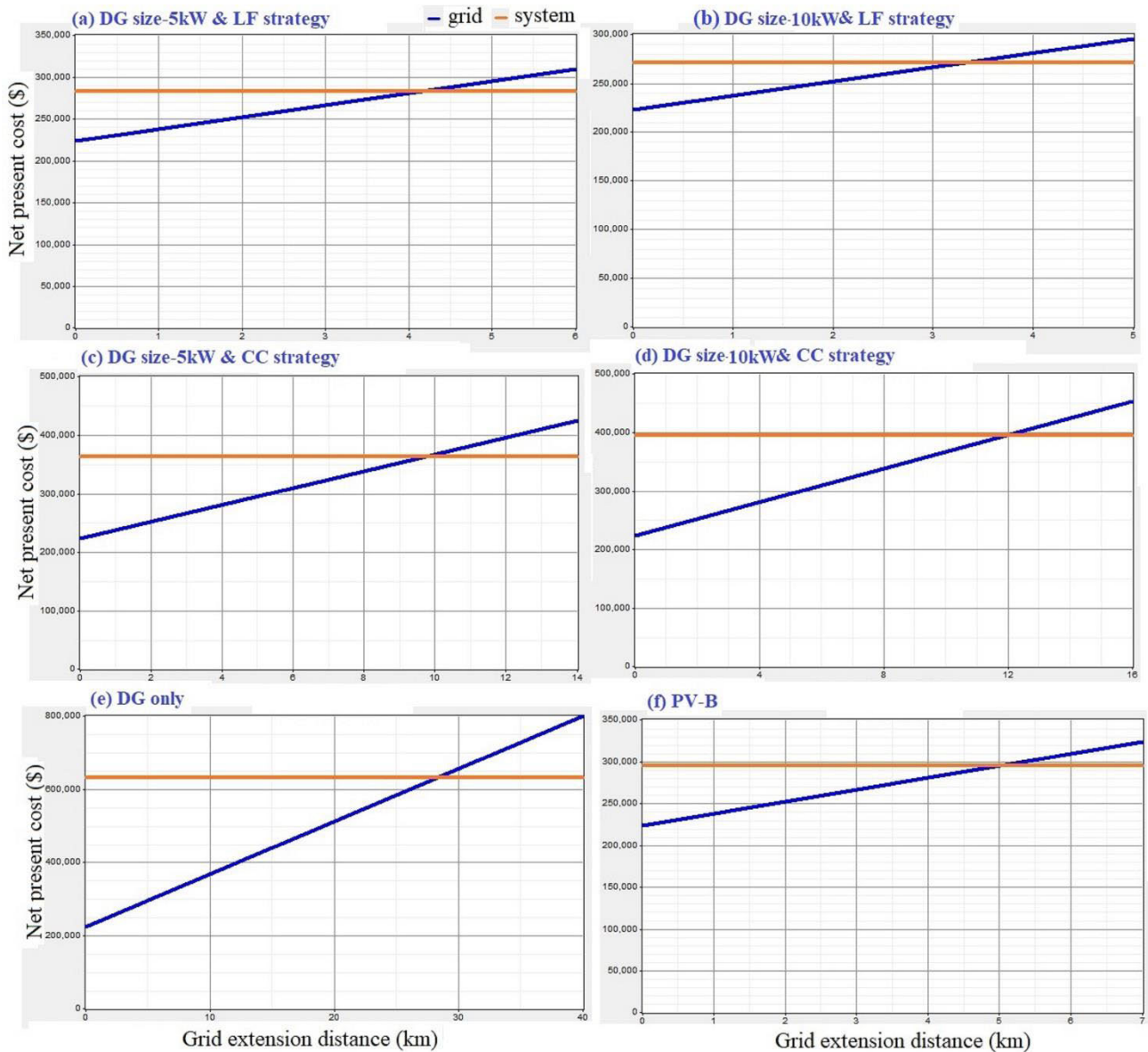
FIGURE 16. Breakeven grid extension distance for different systems. RO-500 unit varying control strategy and size of DG.

case study and the nearest utility grid point (12 km). From Figure 17, it can be concluded that the grid connection is better than all considered cases using the RO-250 unit. For the RO-500 unit, all options of hybrid PV/DG/B are more economically feasible compared with grid connection, and the best cost-effective option is the one including load following control strategy with 10 kW DG. The breakeven distance is 3.31 km.

The initial and replacement cost of the diesel generator is assumed to be $230/kW. Whereas, the O&M cost is considered to be $0.1/h based on an operation lifetime of 15,000 h. The diesel price in Egypt is $0.428/ [55]. However, this value can be increased in the located far regions because of the high transport fee. The optimization results confirmed that

the best size of the DG is 25 kW and 45 kW, respectively, for RO-250 and RO-500. The COE and NPC for DG only with RO-250 are $0.164/kWh and $604298, respectively. Whereas with RO-500, the COE and NPC are $0.171/kWh and $630856, respectively.

From the environmental impact, the stand-alone diesel generator produces 119110 kg/year and 117677 of CO_2 respectively for RO-250 and RO-500. Such quantity can be significantly reduced thanks to PV/DG/B system. Also, the other pollutants were reduced compared to the DG system. Table 11 shows the number of different pollutant emissions by different options of PV/DG/B system compared to DG. Consequently, along with the PV/DG/B system can reduce the CO_2 emission, which affects Global Warming.
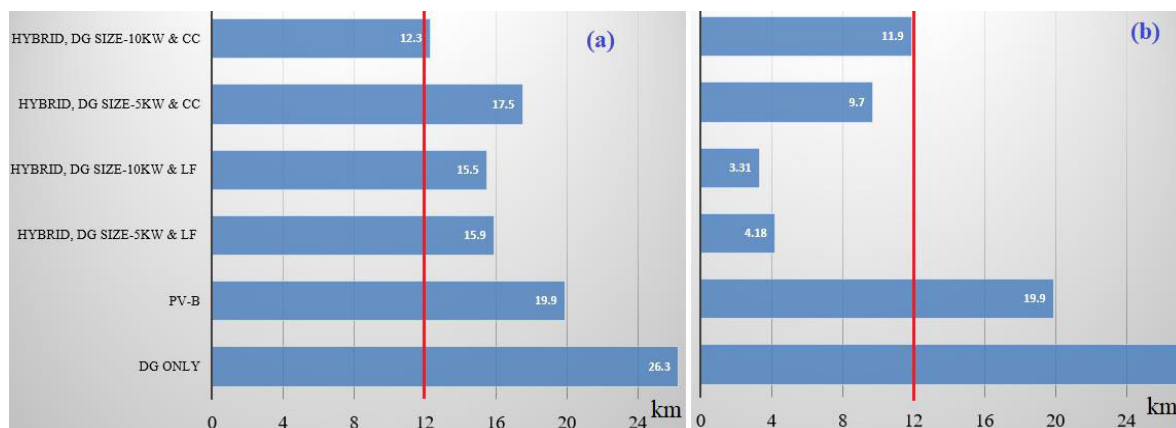
FIGURE 17. Comparison of breakeven grid extension distance under different cases (a) RO-250; (b) RO-500 unit.

TABLE 11. Pollutants emission for different options of PV/DG/B system and stand-alone diesel generator.

Pollutant (kg/year)	DG- only	PV/DG-B			
		RO-250 Unit			
		LF Strategy		CC Strategy	
		DG-5 kW	DG-10 kW	DG-5 kW	DG-10kW
Carbon dioxide	119110	17828	8757	24325	46861
Carbon monoxide	294	44	21.6	60	116
Unburned hydrocarbons	32.6	4.87	2.39	6.65	12.8
Particulate matter	22.2	3.32	1.63	4.53	8.72
Sulfur dioxide	239	35.8	17.6	48.8	94.1
Nitrogen oxides	2623	39.9	193	536	1032
		RO-500 Unit			
		LF Strategy		CC Strategy	
		DG-5 kW	DG-10 kW	DG-5 kW	DG-10kW
Carbon dioxide	117677	5171	8757	22578	34623
Carbon monoxide	290	12.8	21.6	55.7	85.5
Unburned hydrocarbons	32.2	1.41	2.39	6.17	9.47
Particulate matter	21.9	0.962	1.63	4.2	6.44
Sulfur dioxide	236	10.4	17.6	45.3	69.5
Nitrogen oxides	2592	114	193	497	763

VIII. CONCLUSION

Optimization, feasibility, economic evaluation, and energy management of hybrid photovoltaic-diesel-battery (PV/DG/B) system to pump and desalinate water at isolated regions have been done in this paper. The case study represents a flat 70 acres (283280 m^2) located in Minya city (Egypt). The main findings can be summarized as follows;

- From the economic point of view, the minimum cost of energy and the minimum total present cost are 0.074 $/kWh and 207676 $, respectively. This is achieved with RO-500 using load following (LF) dispatch control strategy.
- The related sizes to the best option of PV/DG/B are 120 kW PV array, 10 kW DG, 64 batteries, and 50 kW converter.
- The load following strategy decreased the cost of energy with RO-500 by 22.2% and 31.48% respectively for DG size of 5kW and 10 kW compared with the cycle charging (CC) control strategy.

- The fuel cost records the maximum value of 167737$ using RO-250 with 10 kW of DG and CC strategy. It increased by 92.65% compared with 5 kW of DG and CC strategy.
- The cost of fuel is mainly influenced by the dispatch control strategy. It is equal 123932 $ and 31344 $ respectively for RO-500 with CC and LF strategies with the same size of DG (10 kW). This means that the cost of fuel reduced in the case of LF by 74.71% compared with the CC strategy.
- The grid connection is better than all considered options when using the RO-250 unit.
- For the RO-500 unit, all options of hybrid PV/DG/B are more economically feasible compared with grid connection, and the best cost-effective option is the one including LF strategy with 10 kW DG. The breakeven distance is 3.31 km.
- From the environmental impact, the stand-alone diesel generator produces 119110 kg/year and 117677 kg/year

of CO_2 respectively for RO-250 and RO-500. This can be significantly reduced thanks to PV/DG/B system.

- Along with the PV/DG/B system being more economical, the CO_2 emission, which affects Global Warming, is reduced.

REFERENCES

[1] (2030). *Egypt Vision*. Accessed: Mar. 21, 2020. [Online]. Available: https://www.arabdevelopmentportal.com/

[2] IRENA. (2018). *Renewable Energy Outlook: Egypt. International Renewable Energy Agency*. Abu Dhabi. Accessed: Mar. 21, 2020. [Online]. Available: https://irena.org/publications/2018/Oct/Renewable-Energy-Outlook-Egypt

[3] D. Fernandez-Cerero, A. Fernandez-Montes, and A. Jakobik, "Limiting global warming by improving data-centre software," *IEEE Access*, vol. 8, pp. 44048–44062, 2020, doi: 10.1109/ACCESS.2020.2978306.

[4] N. Bizon, N. M. Tabatabaei, F. Blaabjerg, and E. Kurt, *Energy Harvesting and Energy Efficiency: Technology, Methods, and Applications*. Cham, Switzerland: Springer, 2017, doi: 10.1007/978-3-319-49875-1.

[5] *Egyptian Electricity Holding Company Annual Report 2015/2016*. Accessed: Mar. 21, 2020. [Online]. Available: http://www.moee.gov.eg/

[6] F. M. Enescu, N. Bizon, A. Onu, M. S. Răboacă, P. Thounthong, A. G. Mazare, and G. Şerban, "Implementing blockchain technology in irrigation systems that integrate photovoltaic energy generation systems," *Sustainability*, vol. 12, no. 4, p. 1540, Feb. 2020, doi: 10.3390/su12041540.

[7] S. Mandal, B. K. Das, and N. Hoque, "Optimum sizing of a stand-alone hybrid energy system for rural electrification in bangladesh," *J. Cleaner Prod.*, vol. 200, pp. 12–27, Nov. 2018, doi: 10.1016/j.jclepro.2018.07.257.

[8] A. Alkaisi, R. Mossad, and A. Sharifian-Barforoush, "A review of the water desalination systems integrated with renewable energy," *Energy Procedia*, vol. 110, pp. 268–274, Mar. 2017, doi: 10.1016/j.egypro.2017.03.138.

[9] V. G. Gude, *Renewable Energy Powered Desalination Handbook: Application and Thermodynamics*. Amsterdam, The Netherlands: Elsevier, 2018, doi: 10.1016/B978-0-12-815244-7.00004-0.

[10] D. Xevgenos, K. Moustakas, D. Malamis, and M. Loizidou, "An overview on desalination and sustainability: Renewable energy-driven desalination and brine management," *Desalination Water Treat.*, vol. 57, no. 5, pp. 14–2304, 2016, doi: 10.1080/19443994.2014.984927.

[11] N. Bizon, "Hybrid power systems," in *Optimization of the Fuel Cell Renewable Hybrid Power Systems*. (Green Energy and Technology). Cham, Switzerland: Springer, 2020, doi: 10.1007/978-3-030-40241-9_2.

[12] N. M. Tabatabaei, E. Kabalci, and N. Bizon, "Overview of microgrid," in *Microgrid Architectures, Control and Protection Methods* (Power Systems), N. M. Tabatabaei, E. Kabalci, and N. Bizon, Cham, Switzerland: Springer, 2020, doi: 10.1007/978-3-030-23723-3_1.

[13] L. Olatomiwa, S. Mekhilef, M. S. Ismail, and M. Moghavvemi, "Energy management strategies in hybrid renewable energy systems: A review," *Renew. Sustain. Energy Rev.*, vol. 62, pp. 821–835, Sep. 2016, doi: 10.1016/j.rser.2016.05.040.

[14] N. Bizon, *Optimization of the Fuel Cell Renewable Hybrid Power Systems*. New York, NY, USA: Springer, 2020, doi: 10.1007/978-3-030-40241-9.

[15] A. Aziz, M. Tajuddin, M. Adzman, M. Ramli, and S. Mekhilef, "Energy management and optimization of a PV/Diesel/Battery hybrid energy system using a combined dispatch strategy," *Sustainability*, vol. 11, no. 3, p. 683, Jan. 2019, doi: 10.3390/su11030683.

[16] H. Rezk, E. T. Sayed, M. Al-Dhaifallah, M. Obaid, A. H. M. El-Sayed, M. A. Abdelkareem, and A. G. Olabi, "Fuel cell as an effective energy storage in reverse osmosis desalination plant powered by photovoltaic system," *Energy*, vol. 175, pp. 423–433, May 2019, doi: 10.1016/J.ENERGY.2019.02.167.

[17] A. Nasr EL-Deen Mourad, A. A. Elbaset, and H. A. Ziedan, "Optimization of PV/Wind power system case study: Supplying large industry load in egypt," *J. Eng. Appl. Sci.*, vol. 15, no. 4, pp. 1014–1020, Nov. 2020, doi: 10.36478/jeasci.2020.1014.1020.

[18] L. M. Halabi, S. Mekhilef, L. Olatomiwa, and J. Hazelton, "Performance analysis of hybrid PV/diesel/battery system using HOMER: A case study sabah, malaysia," *Energy Convers. Manage.*, vol. 144, pp. 322–339, Jul. 2017, doi: 10.1016/j.enconman.2017.04.070.

[19] M. Ansong, L. D. Mensah, and M. S. Adaramola, "Techno-economic analysis of a hybrid system to power a mine in an off-grid area in ghana," *Sustain. Energy Technol. Assessments*, vol. 23, pp. 48–56, Oct. 2017, doi: 10.1016/j.seta.2017.09.001.

[20] S. Ghaem Sigarchian, R. Paleta, A. Malmquist, and A. Pina, "Feasibility study of using a biogas engine as backup in a decentralized hybrid (PV/wind/battery) power generation system—Case study kenya," *Energy*, vol. 90, pp. 1830–1841, Oct. 2015, doi: 10.1016/j.energy.2015.07.008.

[21] H. Rezzouk and A. Mellit, "Feasibility study and sensitivity analysis of a stand-alone photovoltaic-diesel-battery hybrid energy system in the north of algeria," *Renew. Sustain. Energy Rev.*, vol. 43, pp. 1134–1150, Mar. 2015, doi: 10.1016/j.rser.2014.11.103.

[22] M. Madziga, A. Rahil, and R. Mansoor, "Comparison between three off-grid hybrid systems (solar photovoltaic, diesel generator and battery storage system) for electrification for gwakwani village, south africa," *Environments*, vol. 5, no. 5, p. 57, May 2018, doi: 10.3390/environments5050057.

[23] S. Upadhyay and M. P. Sharma, "Development of hybrid energy system with cycle charging strategy using particle swarm optimization for a remote area in india," *Renew. Energy*, vol. 77, pp. 586–598, May 2015, doi: 10.1016/j.renene.2014.12.051.

[24] N. Bizon and P. Thounthong, "Energy efficiency and fuel economy of a fuel cell/renewable energy sources hybrid power system with the load-following control of the fueling regulators," *Mathematics*, vol. 8, no. 2, p. 151, Jan. 2020, doi: 10.3390/math8020151.

[25] H. Rezk, M. Alghassab, and H. A. Ziedan, "An optimal sizing of stand-alone hybrid PV-fuel cell-battery to desalinate seawater at saudi NEOM city," *Processes*, vol. 8, no. 4, p. 382, Mar. 2020, doi: 10.3390/pr8040382.

[26] O. Krishan and S. Suhag, "Power management control strategy for hybrid energy storage system in a grid-independent hybrid renewable energy system: A hardware-in-loop real-time verification," *IET Renew. Power Gener.*, vol. 14, no. 3, pp. 454–465, Feb. 2020, doi: 10.1049/iet-rpg.2019.0578.

[27] A. S. Aziz, M. F. N. Tajuddin, M. R. Adzman, A. Azmi, and M. A. M. Ramli, "Optimization and sensitivity analysis of standalone hybrid energy systems for rural electrification: A case study of iraq," *Renew. Energy*, vol. 138, pp. 775–792, Aug. 2019, doi: 10.1016/j.renene.2019.02.004.

[28] Z. Zhou, C. Wang, and G. E. Leijiao, "Operation of stand-alone microgrids considering the load following of biomass power plants and the power curtailment control optimization of wind turbines," *IEEE Access*, vol. 7, pp. 186115–186125, 2019, doi: 10.1109/ACCESS.2019.2958678.

[29] B. K. Das, Y. M. Al-Abdeli, and G. Kothapalli, "Optimisation of stand-alone hybrid energy systems supplemented by combustion-based prime movers," *Appl. Energy*, vol. 196, pp. 18–33, Jun. 2017, doi: 10.1016/j.apenergy.2017.03.119.

[30] S. Nasri, B. S. Sami, and A. Cherif, "Power management strategy for hybrid autonomous power system using hydrogen storage," *Int. J. Hydrogen Energy*, vol. 41, no. 2, pp. 857–865, Jan. 2016, doi: 10.1016/j.ijhydene.2015.11.085.

[31] S. Upadhyay and M. P. Sharma, "Selection of a suitable energy management strategy for a hybrid energy system in a remote rural area of India," *Energy*, vol. 94, pp. 352–366, Jan. 2016, doi: 10.1016/j.energy.2015.10.134.

[32] M. H. Athari and M. M. Ardehali, "Operational performance of energy storage as function of electricity prices for on-grid hybrid renewable energy system by optimized fuzzy logic controller," *Renew. Energy*, vol. 85, pp. 890–902, Jan. 2016, doi: 10.1016/j.renene.2015.07.055.

[33] J. Pascual, J. Barricarte, P. Sanchis, and L. Marroyo, "Energy management strategy for a renewable-based residential microgrid with generation and demand forecasting," *Appl. Energy*, vol. 158, pp. 12–25, Nov. 2015, doi: 10.1016/j.apenergy.2015.08.040.

[34] S. Berrazouane and K. Mohammedi, "Parameter optimization via cuckoo optimization algorithm of fuzzy controller for energy management of a hybrid power system," *Energy Convers. Manage.*, vol. 78, pp. 652–360, Feb. 2014, doi: 10.1016/j.enconman.2013.11.018.

[35] N. Karami, N. Moubayed, and R. Outbib, "Energy management for a PEMFC-PV hybrid system," *Energy Convers. Manage.*, vol. 82, pp. 154–168, Jun. 2014, doi: 10.1016/j.enconman.2014.02.070.

[36] M. Ismail, M. Moghavvemi, and T. Mahlia, "Techno-economic analysis of an optimized photovoltaic and diesel generator hybrid power system for remote houses in a tropical climate," *Energy Convers. Manage.*, vol. 69, pp. 73–163, May 2013, doi: 10.1016/j.enconman.2013.02.005.

[37] M. Dahmane, J. Bosche, A. El-Hajjaji, and M. Dafarivar, "Renewable energy management algorithm for stand-alone system," in *Proc. Int. Conf. Renew. Energy Res. Appl. (ICRERA)*, Oct. 2013, pp. 621–626, doi: 10.1109/ICRERA.2013.6749830.

[38] D. Feroldi, L. N. Degliuomini, and M. Basualdo, "Energy management of a hybrid system based on wind-solar power sources and bioethanol," *Chem. Eng. Res. Design*, vol. 91, no. 8, pp. 1440–1455, Aug. 2013, doi: 10.1016/j.cherd.2013.03.007.

[39] Y.-K. Chen, Y.-C. Wu, and C.-C. Y.-S. Song Chen, "Design and implementation of energy management system with fuzzy control for DC microgrid systems," *IEEE Trans. Power Electron.*, vol. 28, no. 4, pp. 1563–1570, Apr. 2013, doi: 10.1109/TPEL.2012.2210446.

[40] B. Robyns, A. Davigny, and C. Saudemont, "Methodologies for supervision of hybrid energy sources based on storage systems—A survey," *Math. Comput. Simul.*, vol. 91, pp. 52–71, May 2013, doi: 10.1016/j.matcom.2012.06.014.

[41] A. Basnet and J. Zhong, "Integrating gas energy storage system in a peer-to-peer community energy market for enhanced operation," *Int. J. Electr. Power Energy Syst.*, vol. 118, Jun. 2020, Art. no. 105789, doi: 10.1016/J.Ijepes.2019.105789.

[42] M. J. Mayer, A. Szilágyi, and G. Gróf, "Environmental and economic multi-objective optimization of a household level hybrid renewable energy system by genetic algorithm," *Appl. Energy*, vol. 269, Jul. 2020, Art. no. 115058, doi: 10.1016/J.Apenergy.2020.115058.

[43] N. Tutkun and N. Celebi, "An improved approach to minimise energy cost in a small wind-photovoltaic hybrid system," in *Proc. Int. Renew. Sustain. Energy Conf. (IRSEC)*, Nov. 2016, pp. 858–862, doi: 10.1109/IRSEC.2016.7983981.

[44] NASA. *Surface Meteorology and Energy*. Accessed: Mar. 21, 2020. [Online]. Available: https://power.larc.nasa.gov

[45] *Egypt Solar Atlas*. Accessed: Mar. 21, 2020. [Online]. Available: https://globalsolaratlas.info/

[46] H. Rezk and G. M. Dousoky, "Technical and economic analysis of different configurations of stand-alone hybrid renewable power systems—A case study," *Renew. Sustain. Energy Rev.*, vol. 62, pp. 941–953, Sep. 2016, doi: 10.1016/j.rser.2016.05.023.

[47] H. Rezk and M. Shoyama, "Techno-economic optimum sizing of stand-alone photovoltaic/fuel cell renewable system for irrigation water pumping applications," in *Proc. IEEE Int. Conf. Power Energy (PECon)*, Dec. 2014, pp. 182–186, doi: 10.1109/PECON.2014.7062437.

[48] *MAK Water*. Accessed: Mar. 21, 2020. [Online]. Available: https://www.makwater.com.au/products/sea-water-reverse-osmosis/

[49] H. Rezk, M. A. Abdelkareem, and C. Ghenai, "Performance evaluation and optimal design of stand-alone solar PV-battery system for irrigation in isolated regions: A case study in al minya (Egypt)," *Sustain. Energy Technol. Assessments*, vol. 36, Dec. 2019, Art. no. 100556, doi: 10.1016/j.seta.2019.100556.

[50] A. Askarzadeh, "Distribution generation by photovoltaic and diesel generator systems: Energy management and size optimization by a new approach for a stand-alone application," *Energy*, vol. 122, pp. 542–551, Mar. 2017, doi: 10.1016/j.energy.2017.01.105.

[51] K. Sayed, M. G. Gronfula, and H. A. Ziedan, "Novel soft-switching integrated boost DC-DC converter for PV power system," *Energies*, vol. 13, no. 3, p. 749, Feb. 2020, doi: 10.3390/EN13030749.

[52] M. Abdel-Salam, A. Ahmed, H. Ziedan, K. Sayed, M. Amery, and M. Swify, "A solar-wind hybrid power system for irrigation in toshka area," in *Proc. IEEE Jordan Conf. Appl. Electr. Eng. Comput. Technol. (AEECT)*, Dec. 2011, pp. 6–8, doi: 10.1109/AEECT.2011.6132491.

[53] B. K. Das, N. Hoque, S. Mandal, T. K. Pal, and M. A. Raihan, "A techno-economic feasibility of a stand-alone hybrid power generation for remote area application in bangladesh," *Energy*, vol. 134, pp. 775–788, Sep. 2017, doi: 10.1016/j.energy.2017.06.024.

[54] *Egyptian Ministry of Electricity and Renewable Energy*. Accessed: Mar. 21, 2020. [Online]. Available: http://www.moee.gov.eg/

[55] *Egyptian Ministry of Petroleum and Mineral Resources*. Accessed: Mar. 21, 2020. [Online]. Available: https://www.petroleum.gov.eg/

• • •